Lidar-Aided Measurement of Phytoplankton Chlorophyll and Underwater Scattering Layers

A.F. Bunkin and A.L. Surovegin

Institute of General Physics, USSR Academy of Sciences, Vavilova 38, 117942, Moscow, USSR
RADIAN R&D Centre, P.O. box 1929 Moscow 129010, USSR

ABSTRACT

Mapping of phytoplankton chlorophyll content as well as of underwater scattering layers was done using both airborne and shipborne lidar detection. Field experiments were run in the Atlantic and Pacific Oceans and the Mediterranean, Baltic and Caspian seas, Arctic area. Thermal stratification was proved to exist throughout the sea depth by the use of a submersible sensor.

INTRODUCTION

One of the most important problems the modern environmental science encounts and identification of various impurities in the ocean. Sources of impurities in sea water are diverse, the most common of them being transport, agriculture, oil industry any accidental spills. Once ecological balance is disturbed, biological processes in sea water become affected, the result being altered chlorophyll concentrations, turbidity, water temperature changes etc.

During the last eight a number of new remote sensing methods (e.g. based on nonlinear laser spectroscopy) were developed at the Institute of General Physics. We have created new types of lidars and arranged nearly ten aircraft and shipboard expenditioins. Some aircraft expeditions dealt with terrestrial investigations, e.g. of vegetation and mineral fluorescence. Others were devoted to oceanological research, the results of which the are subject of this paper.

1. EQUIPMENT

During eight years of R&D endeavour concerned with laser-aided remote sensing we created five different types of lidars, three shipboards ones, of which two are designed for chlorophyll and oil slick detection and one for studying underwater scattering layers, and two lidars for airborne ivestigations, namely, a fluorescence lidar (intended, apart from oceanology, for geological and agricultural experiments) and a depth sounder.

Let us consider the last two devices (shown in Figs.1 and 2).

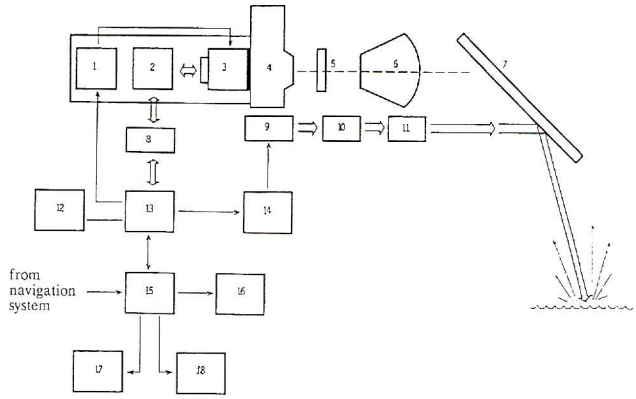

Fig. 1 - Lidar Fluorosensor: 1 high voltage strobe pulse forming - 2 CCD array electronic support - 3 image intensifier - 4 polychromator - 5 glass filter - 6 collector objective - 7 folding mirror - 8 interface - 9 laser - 10 second harmonic generator - 11 third or fourth harmonic generator - 12, 16 hard and floppy disc memory - 13, 15 personal computers - 14 laser power supply - 17 data bank - 18 hard copy.

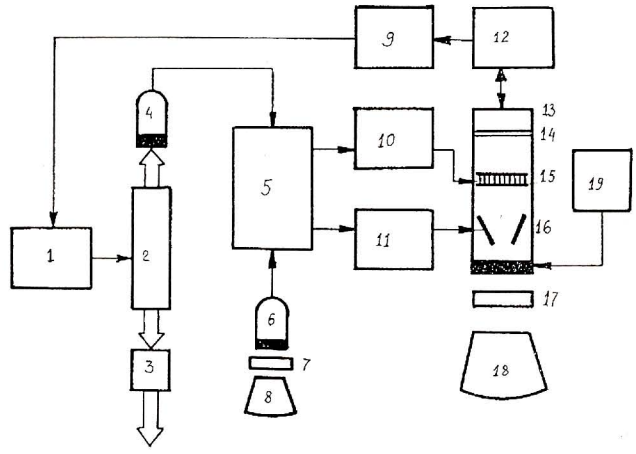

Fig. 2 - Laser depth sounder: 1 laser power supply - 2 ND:YAG laser - 3 frequency doubler - 4, 6, photomultiplayers - 5 automatic measurement of delay - 7 passive filter - 8 objective - 9 computer - 10 high voltage pulser - 11 sweep pulser - 12 interface - 13 CCD - 14 image intensifier - 15 MOP - 16 deflecting plates - 17 passive filter - 18 objective - 19 high voltage supply

The both are exicited by a high-power Nd:YAG laser with the second and fourth harmonic oscillators (for depth sounding, only the second harmonic is used). The frequency-doubled laser output provides FWHM 8ns pulses with pulse energy of 200-300mJ and repetition rate of 10-20 pulses/s. The beam diameter at the telescope output (after beam expansion) is 4 cm, and divergence makes 0.20mrad. As a result, at a distance of 500m from the source (typical target distance for airborne experiments), the beam diameter is about 20cm. The receiving telescope is of Newtonian design, the diameter being 40 or 20cm for airborne or shipborne lidars, respectively. At the focal point, the light is collected by the entrance slit of a spectrum (for the fluorescence lidar) or time (for the depth sounder) analyzer. Spectrum dispersion is provided by a polychromator, while time dispersion is enabled by a streak camera with a multichannel plate (MCP) intensifier. The polychromator provides two bandwidths of 250nm and 500nm that can be shifted, if desired. The depth sounder streak camera (Fig.2) is triggered by a laser pulse and an optical pulse coming from the sea surface. Then, after the delay automatic measurement, a high voltage pulse and a sweep pulse are generated and sent to the streak camera. The resulting temporal image is ready by a CCD array, whereupon it is set, individually for each laser pulse, into an IBM PC/XT microcomputer and stored on a hard disc. The spectral image is then ready by an O.M.A. detector with an MCP and a CCD-array receiver (Fig.1).

2. DETECTION OF PHYTOPLANKTON CHLOROPHYLL AND HYDROCARBONS IN SEA WATER

Phytoplankton sensing is carried out primarly with the object of determining concentration, functional condition as well as species composition of algae. In our field experiments, we studied the former topic using sounding technique to estimate temporal and spatial distributions of chlorophyll "a" in the Mediterranean, Baltic, Caspian, Black seas and the Sea of Japan. The technique is based on measurement and mapping of the ϕ parameter of chl "a", $\phi = [I(f)/I(r)]$, where I(f) is chl "a" fluorescence intensity in non-saturation conditions and I(r) is water Raman scattering intensity taken as a reference signal. The sensing means used for these studies was a fluorescence lidar.

The data were acquired during 6 shipboard and 4 aircraft expeditions. The sounding distances were 20-30m in shipboard and 500-800m in airborne measurements. Fig.3 presents an example of divostok (summer of 1988). The chl "a" concentration can be calculated from this spectrum by comparison with the spectrum of an in vitro grown net algae whose chl "a" content is known.

Calculated concentrations was 5mg/l, while biological test results suggested it to be 3 mg/1. Clearly very tiny cells had not been captured by plankton.

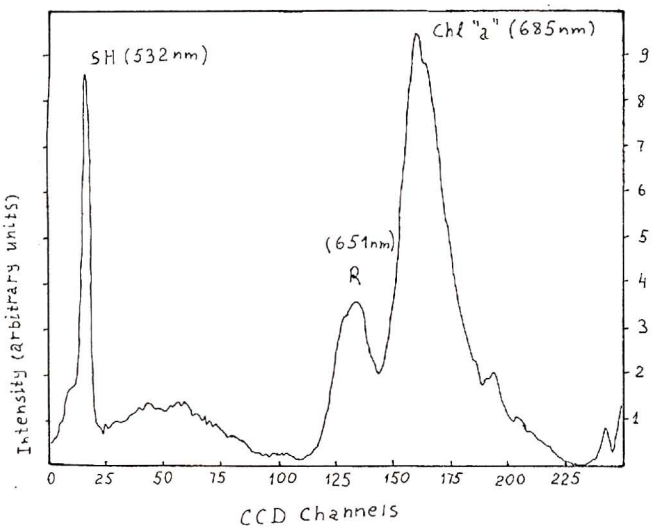

Fig. 3 - Echo-signal spectrum of sea surface in Vladivostok harbor, which was excited by second harmonic of Nd:YAG laser.

Of further interest was to determine oil pollution sites and to distinguish spectra of oil and gelbstoff containing waters. Our experience suggested that the simplest method to solve these problems is by the means of remote sensing employing the fourth harmonic of the Nd:YAG laser (266 nm) as excitation source. Fig. 4 demonstrates fluorescence spectra of sea surface water obtained using this means. One can see that gelgstoff and crude oil have peaks at wavelengths 420 nm and 340 nm, respectively.

Fig. 5 shows chl "a" and gelbstoff distribution in coastal waters nearby the Gelenjik harbour in the Black sea. Chl "a" concentration varies aound 0.3 mg/1 (k=0.4), while that of gelbstoff varies either in line with it or in quite a reverse mode (as indicated by arrows).

During the field experiments we came upon an oil slick. Shown in Fig. 6 is the relevant echo-signal spectrum and parameter k temporal variation indicating decay of hydrocarbon concentration on the sea surface.

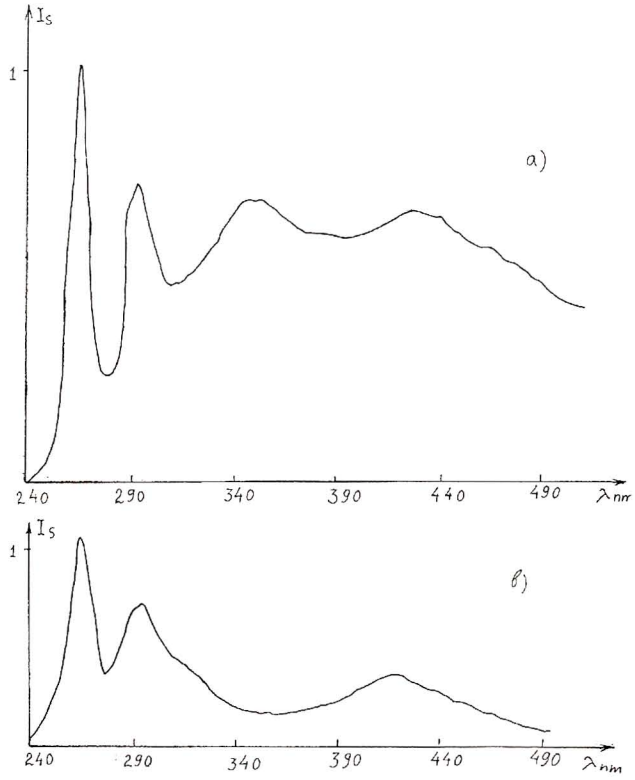

Fig. 4 - Fluorescence spectra of sea surface, which were excited by 266nm radiation. a) Novorosiisk, Oil terminal b) Gelenjik, Blue harbor.

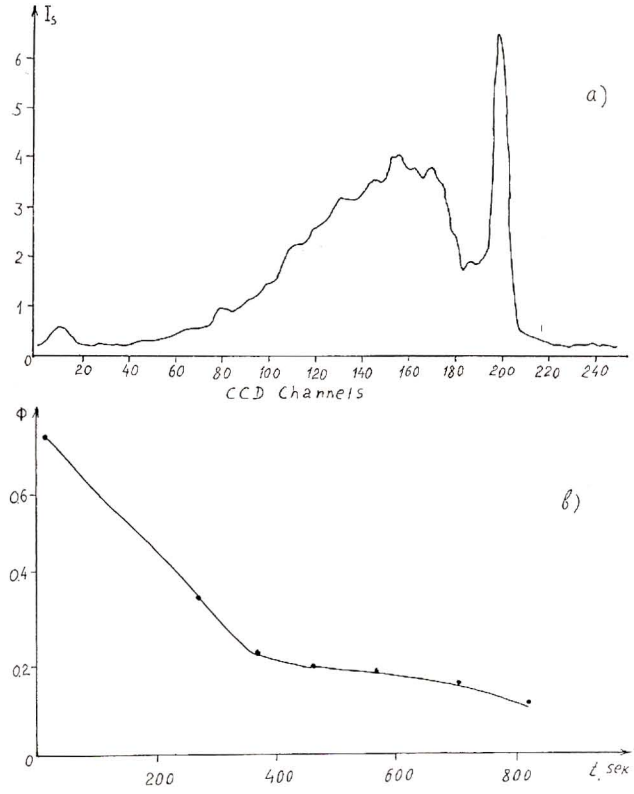

Fig. 6 - Echo-signal spectrum (a) and temporal variation of parameter F (b), which reflects the surface concentrations of hydrocarbons.

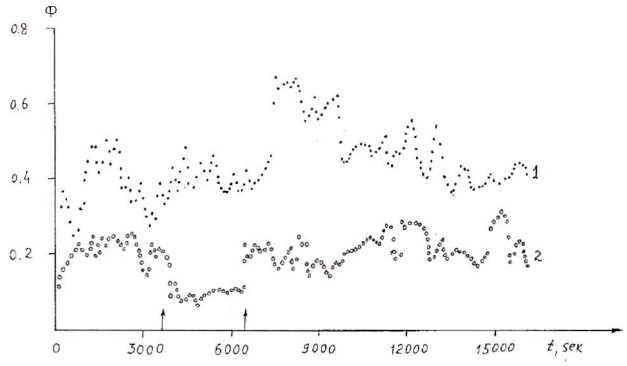

Fig. 5 - Chlorophyll "a" (1) and gelbstoff (2) distribution at the coastal zone of Black Sea near Gelenijk and Novorosiik. Start point is 44, 5 N, 37, 600; finish point is 44, 60N, 38, 200.

3. LIDAR SENSING OF UNDERWATER SCATTERING LAYERS

Airborne and shipborne lidar detection and mapping of underwater scattering layers is a promising area of laser remote sensing technique applications. Experiments were carried out using a bathymetric lidar shown in Fig. 5 in the Black sea and the Atlantic and Arctic oceans. Deep-water and sea bottom temperature profiles were acquired by launching a submersible sensor from aboard a ship. Some results of these experiments are presented in Figs. 7, 8.

Fig. 7 shows results of temperature measurements and backscattered laser light intensity versus depth for a West Atlantic region, 36N, 63W (September 1989). Measurement noise is neglected in the plot.

These data are the result of 700 laser shots averaging, and the depth was calculated by the delay of the sea surface backscattered pulse. The comparison of the temperature data with those on backscattered radiation suggests a close correlation between these environmental parameters. For all shipborne lookout stations in the region, we observed

an increase of backscattering intensity at the thermocline depth. To make sure that this feature was not associated with any apparatus effects, we displaced the scanned area both up and down by changing the depth sounder's sync pulse delay.

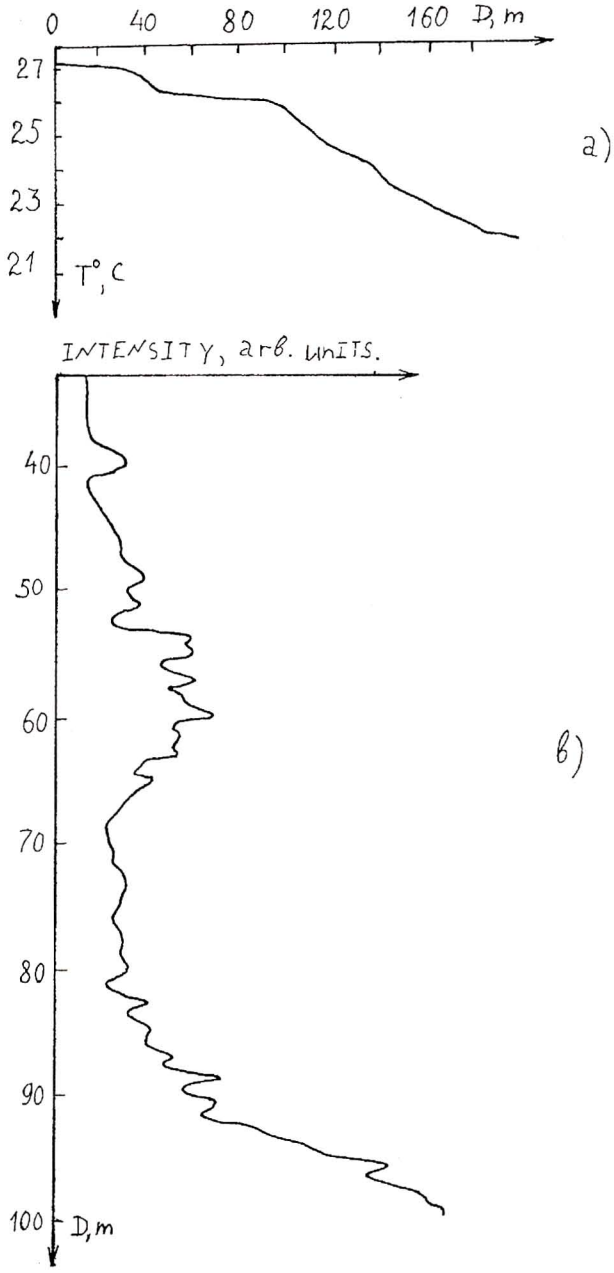

Fig. 7 - Temperature (a) and laser light backscattering (b) depth distribution. Atlantic Ocean, september 1989, 36N, 630W.

Fig. 8 shows results of airborne depth sounding carried out in the summer of 1985 in the Arctic, namely, in the Ob delta, which is an important navigation region because of intensive oil equipment carriage to the West-Siberia oil fields. We acquired a number of bathymetric profiles while the ship was underway. At this time of the year of the Ob delta water is turbid, which fact restricted the sounding depth to 25-30m. Fig. 8 illustrates a good agreement between lidar and standard shipboard sonar data. The difference in depths for shallows can be attributed to variations of bottom profile along the river bed.

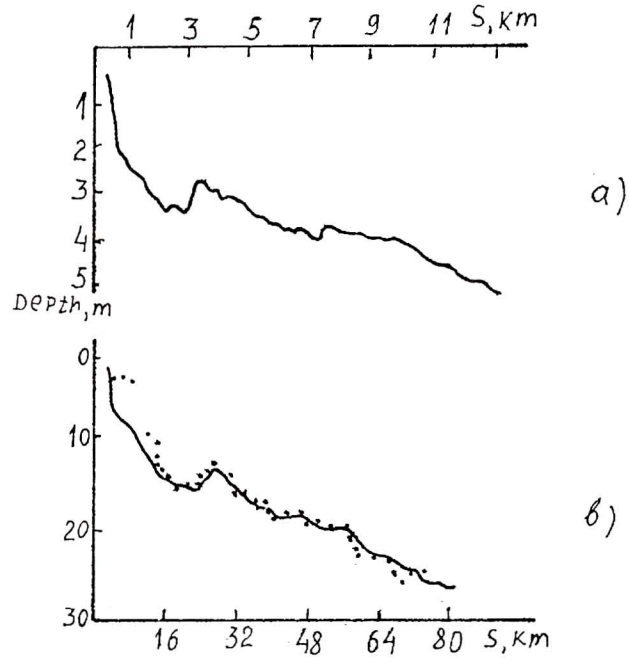

Fig. 8 - Airborne laser depth sounding. Arctic Ocean, Ob River delta, July 1985. a)Depth profile acquired by laser system. b) solid line-laser depth sounding, points - standard shipboard sonar measurements.

4. SUMMARY AND CONCLUSIONS

A number of lidar systems for chlorophyll "a" and hydrocarbons monitoring and depth sounding were created and tasted during several years of field experiments. The data on temporal and spatial variations of chl "a", gelbstoff and hydrocarbons concentrations were obtained in the harbours of Varna, Vladivostok, Petropavlovsk, Sevastopol, Novorossijsk, Gelenijk as well as on the open Black, Baltic, Japan, Bering, Caspian and Mediterranean seas.

Backscattered laser light from underwater layers and sea bottom was captured from down to 100m. Bathymetric profiles were taken in the Arctic, across tested areas.

Work on further modification of lidar systems is currently underway. Instruments under development are expected to reduce Frensel backscattering from sea surface and to improve the S/N ratio. The efficiency of these new systems is to be tested by future field experiments.

The authors thank all those who by taking part in field experiments, research ship expeditions and aircraft operations promoted this study.

REFERENCES

Bunkin A.F., Galumyan A.S., Mal'tsev D.V., 1986, Nonlinea polarization remote Raman spectroscopy. JETP Letters, 43, 43-46.

Bunkin A.F., 1988 In: Laser Physics and Applications, Singapore, New Jersy, London: World Scientific, Ed: A.Y. Spasov, 646-665.

Bunkin A.F., Vlasov D.V., Galumyan A.S., Sursky K.O., 1987 In: "Oceanic Remote Sensing" (N.Y.: Nova Science Publishers, Eds. F.V. bunkin and K.I. Voliak), 74-88.

Abroskin A.G., Bunkin A.F., Vlasov D.V., Gorbunov A.L., Mirkamilov D.M. 1987 In: "Oceanic Remote Sensing" (N.Y.: Nova Science Publishers, Eds. F.V. Bumkin and K.I. Voliak), 32-52.

Bunkin A.F., Vlasov D.V., Mirkamilov D.M. 1987, Physical Principles of Airborne Laser Remote Sensing (Tashkent: FAN).

Bunkin A.F., Surovegin A.L. 1986, Remote detection of chlorophyll using laser-induced fluorescence method. Oceanology, 31, 532-36.

Bunkin A.F., Vlasov D.V., Galumyan A.S., Mal'tsev D.V., Mirkamilov D.M., Slobodianin V.P. 1984, Airborne laser system for remote sensing of atmosphere, ocean and vegetation. Journal of Technical Physics (Sov.), 54, 2190-2195.

Bunkin A.F., Vlasov D.V., Rezov A.V., Tsipenyuk D.YU. 1990, Observation of the laser-beam reflection from inner oceanic scattering layers. Fifteenth International Laser Radar Conference. Abstract of papers, Part 2, 71-74.